Composites Part C: Open Access 3 (2020) 100048

Contents lists available at ScienceDirect

Composites Part C: Open Access

journal homepage: www.elsevier.com/locate/jcomc

A novel sandwich panel made of prepreg flax skins and bamboo core

Lívia Ávila de Oliveira[a,b], Gabriela Luiza Cota Coura[a], Maikson Luiz PassaiaTonatto[c], Túlio Hallak Panzera[a,b,*], Vincent Placet[d], Fabrizio Scarpa[e]

[a] Centre for Innovation and Technology in Composite Materials – CITeC, Department of Mechanical Engineering - PPMEC, Federal University of São João del Rei-UFSJ, São João del Rei, Brazil
[b] Department of Natural Sciences - FQMat, Federal University of São João del Rei-UFSJ, Brazil
[c] Group on Mechanics of Materials and Structures - GMEC, Federal University of Santa Maria – UFSM, Cachoeira do Sul, Brazil
[d] Department of Applied Mechanics, Université Bourgogne Franche-Comté, FEMTO-ST Institute, CNRS/UFC/ENSMM/UTBM, 25000 Besançon, France
[e] Bristol Composites Institute - ACCIS, University of Bristol, BS8 1TR Bristol, UK

ARTICLE INFO

Keywords:
Sandwich panel
Flax fibre
Bamboo
Thermosetting
Flexural and shear properties

ABSTRACT

This work describes the bending and shear mechanical properties of a novel concept of sustainable sandwich panel made from unidirectional prepreg flaxtape skins and bamboo rings as a circular core material. A Design of Experiment (DoE) is used to determine the influence of the bamboo diameter and the type of adhesive bonding between core and skins on the equivalent density, flexural and shear properties of these panels. Numerical analysis are also performed using cohesive surface contacts between skins and bamboo rings to investigate the structural behaviour and failure mechanisms of the sandwich panels. The equivalent density is affected by both factors, with an overall decrease when larger bamboo rings and lower density adhesive are used. Although sandwich panels with the larger bamboo rings as core show superior flexural properties and skin stress, smaller bamboo rings cores shows an increase in the core transverse shear modulus. The physical and mechanical characteristics of the adhesives directly affect the failure mode and the overall structural integrity of the panels.

1. Introduction

Sandwich panels are lightweight structures employed in many engineering applications, such as aerospace and automotive components, military devices and civil infrastructure [1–3]. The advantage of the use of sandwich panels lies in their high energy absorption and outstanding mechanical performance [4–6]. A sandwich panel is composed by two thin, stiff and strong sheets/skins commonly made of metals (steel, aluminium) or polymers (polycarbonate, polypropylene). The skins are separated by a thick core made of thin-walled hexagonal, circular or random shaped cells and low-density material [7,8].

In recent years, the awareness of global environment challenges has led researchers to study alternative materials for the development of sustainable sandwich panels [9–11]. The use of fibrous resources available in agriculture is the most widely explored way of developing those sustainable materials because of their availability and accessibility, biodegradable properties, renewability, low cost, low density and specific mechanical properties for secondary structural applications [12–16].

The use of flax fibres dates back to 5000 BC as the first known fibre extracted from plants to reinforce matrices [17,18]. Currently, flax is the most widely used bio-fibre due to its good mechanical properties and versatility. Flax is also widely available [19]; it can be found in simple household textiles, furnishing fabrics and decoration accessories [20]. Flax has also been developed into prepreg textiles for more technological applications, such as transport, wind energy, sports and leisure [21].

Another natural material that has gained popularity within the scientific community is bamboo. Bamboo has been widely used to build permanent and temporary structures [22]. In addition to all the advantages of bio-based plants, bamboo features a fast growth rate, a high strength-to-weight-ratio, good flexibility and lightweight characteristics that are compatible with engineering requirements for use in civil constructions [23–26]. In addition, the circular geometry of the bamboo stem offers the potential to be used in developing sustainable circular core materials for sandwich structures.

Besides the correct selection of the materials for skins and cores, skin-core bonding is another critical factor that directly affects the mechanical performance of sandwich panels because the adhesion to the

* Corresponding author at: Department of Mechanical Engineering - PPMEC, Federal University of São João del Rei-UFSJ, São João del Rei, Brazil.
E-mail address: panzera@ufsj.edu.br (T.H. Panzera).

https://doi.org/10.1016/j.jcomc.2020.100048
Received 24 July 2020; Received in revised form 22 September 2020; Accepted 28 September 2020

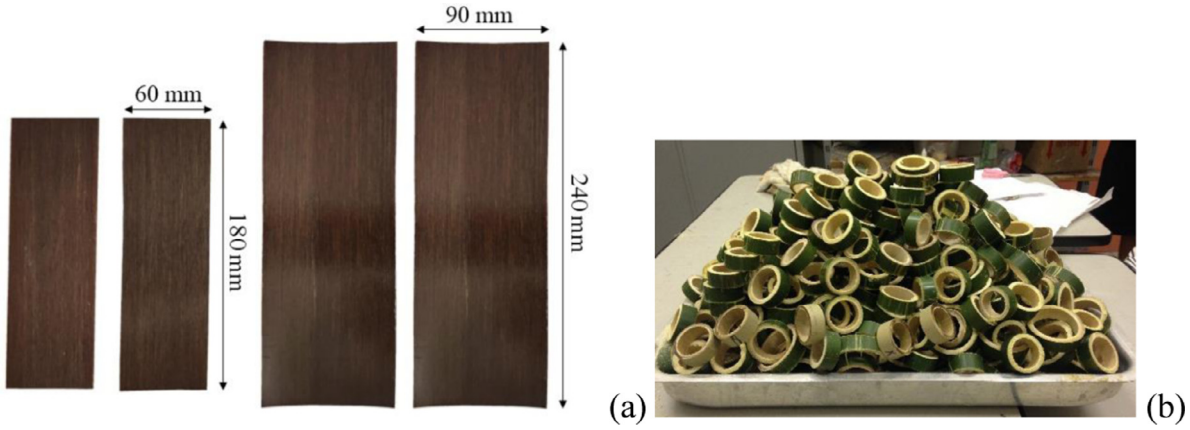

Fig. 1. (a) Skins and (b) core of the sandwich panels.

single sections of the core are the structurally weakest parts of the sandwich [27]. Two types of bonding are commonly used in composite structures: mechanical and adhesive [27]. The adhesive bonding is the most widely used because of the intrinsic low stress concentrations, effective weight reduction, uniform stress and load distribution [28]. The strength of bonded joints depends on several factors, such as the type of the specific joint, its geometric parameters, the bonding materials and the charcateristics of the adhesive [29]. Epoxy adhesives represent the most common type of structural adhesive due to their relatively high modulus and strength [30].

The engineering use of natural or bio/eco-based materials is promising, but unfortunately leads to a variability of the mechanical and physical properties of the structures made of those solids. The scarcity of large datasets of data with statistical robustness also does not help to completely understand the physics and the mechanics underpinning the mechanical behaviour of bio-based structures. A numerical analyses was performed to establish the elastic constants of bamboo structures along their transverse axes [31]. Some studies have used a finite element method based on graded finite elements to obtain orthotropic constitutive properties through the bamboo wall [32,33].

Some experimental and numerical studies related to the flexural properties of sustainable sandwich composites made from a circular bamboo core and biodegradable skins have been investigated recently. Darzi et al. [34] carried out a numerical study on the flexural capacity of ultralight sandwich panels made of plywood faces and bamboo core, using a proposed Ritz method and a validated Finite Element Analysis (FEA). Hartoni et al. [35] investigated, through experimental analysis, the flexural strength of sandwich composites made with bamboo core and multiplex skins, varying the thickness of the core and skin. Loth and Forster [36] developed and characterised a sandwich panel made of bamboo core and glass/flax fibre skins comparing flexural strength with other commercial core materials. In this context, there is much to understand using the bamboo ring as the core material of sandwich panels, e.g. the effects of bamboo species and geometric characteristics, core packing, type of adhesives and skins on different loads and respective failure modes, in addition, to relating the experimental and numerical analysis.

Furthermore, circular cores of bamboo rings lead to a substantial stress concentration in the skins and adhesives under bending loads because of the high strength and stiffness of those rings. The high stress concentrations decrease the structural efficiency of the panels. In order to better understand such effects, two types of adhesives and cell dimensions are also evaluated in this work. The sandwich panels with unidirectional prepreg flax skins and the bamboo core are assessed here by performing a full factorial design of experiment (DoE) and a finite element analysis to better understand the behaviour of the panels under three-point bending tests.

2. Materials and methods

2.1. Materials

The skins of the sandwich panel are made of unidirectional flax fibre reinforced composite (Fig. 1a). The architecture of the uni-directional skin laminate consists in flax fibres pre-impregnated with fire-retardant epoxy polymer XB 3515 GB (Huntsman). The epoxy is also combined with Aradur 1571 BD and Accelerator 1573 BD. The prepreg flaxtape of 220 g/m^2 grammage (fibre+resin) is supplied by EchoTechnilin (Lineo, France), considering an impregnation weight ratio of 50/50 fibre/matrix. A fibre/matrix volume fraction of 56/43% is estimated by analysing the surface of the image obtained by Tescan Mira3 scanning electron microscope operating at 20 kV. The Tescan Essence software is used to recognise and determine the surface area of each constituent.

The core of the sandwich panels is composed of treated bamboo rings (Fig. 1b) approximately 3-years-old, belonging to the *Bambusa tuldoides* species. Bamboo culms are harvested during the waning moon at the Federal University of São João del-Rei campus (Brazil, 21°08′26.5″S 44°15′41.3″W). Boric acid (H_3BO_3, 99%) and copper sulphate ($CuSO_4.5H_2O$, 98.5%) are used for the treatment of the bamboo.

Two different types of polymers are here used as a core-face adhesive: a heat/chemical-resistant epoxy adhesive Araldite 2014 A/B (Huntsman, Araldite AW 139 + hardener XB 5323), with a mixing ratio by weight of 100:50 [37], respectively, and a fire-retardant epoxy system (Sicomin Epoxy Systems, SR1124 resin + SD4775–1 hardener), with a mixing ratio by weight of 100:23 [38], respectively.

2.2. Manufacturing process

2.2.1. Skins

The skins of the sandwich panels are made separately, in three different processes, as recommended by the supplier of prepreg fibres [21]: hand lay-up followed by vacuum compaction and autoclave techniques. Initially, several flax plies are cut from the prepreg roll by scissors according to the sandwich panel dimensions (60 mm × 180 mm and 90 mm × 240 mm), as shown in Fig. 1a. Subsequently, for each skin, three prepreg flax plies are laid up along the unidirectional orientation ($[0]_3$) and wrapped in a release film to prevent leakage of polymer in the autoclave, as shown in Fig. 2a. Prior to the cure, the system is sealed with a breather and a pre-vacuum is applied to compact the samples before being taken to the autoclave, as shown in Fig. 2b. Curing is carried out in an autoclave at a constant pressure of 100 psi (~0.7 MPa) and a temperature ramp of up to 140 °C, keeping the temperatures of 80 °C and 140 °C constant for 100 min. Finally, 0.6 mm thick flax composites are placed in a plastic bag to prevent moisture absorption until the sandwich panel is manufactured.

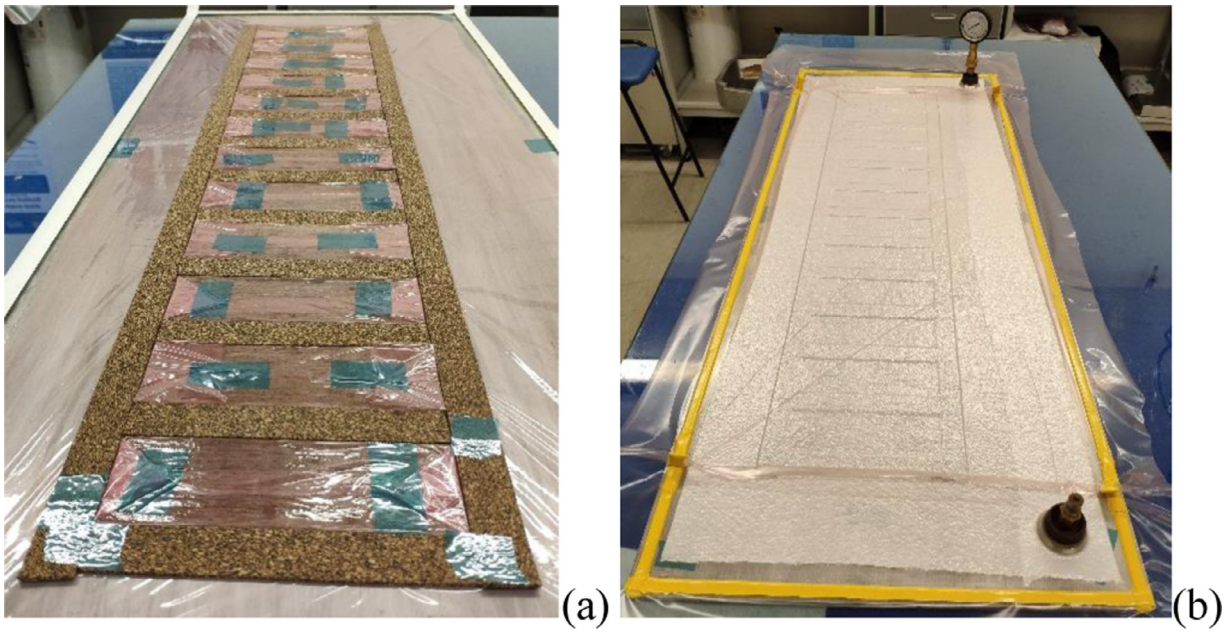

Fig. 2. Manufacturing tehcniques of the skins prior to autoclave: (a) hand lay-up and (b) vacuum compaction.

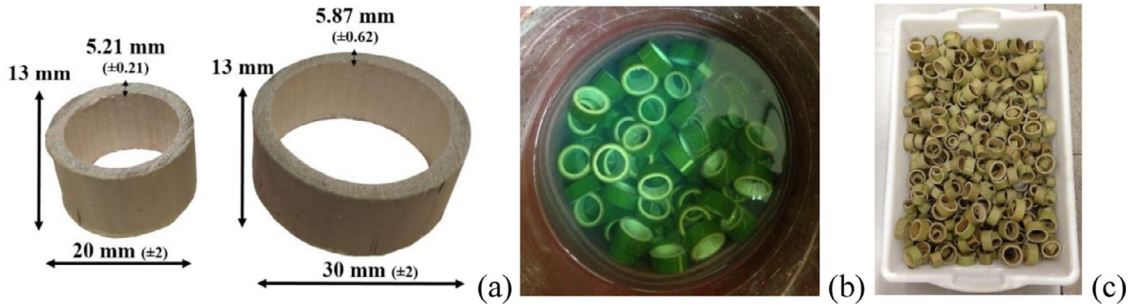

Fig. 3. Bamboo treatment process: (a) dimensions of the cell cores, (b) immersion in solution and (c) drying.

2.2.2. Bamboo treatment

Bamboo culms are harvested and left upright for two weeks to drain and ferment the starch and sugar present in the culms [31]. Subsequently, the bamboo rings are cut by a bandsaw, with the dimensions shown in Fig. 3a. The rings are immersed in a 3% (m/v) boric acid solution and 1% (m/v) copper sulfate for seven days to prevent biological degradation (Fig. 3b). Finally, the bamboo rings are oven dried at 50 °C for three days before being used in the manufacture of the sandwich panels (Fig. 3c).

2.2.3. Sandwich panels

Prior to the sandwich manufacturing, the polymer adhesives are prepared by hand mixing the components for five minutes, i.e., AW 139 + hardener XB 5323, from Huntsman and SR1124 resin + SD4775–1 hardener, from Sicomin. The adhesives are spread separately on the flax skins using a 1.5 mm deep zigzag spatula for the Huntsman adhesive, while a brush is used for the Sicomin polymer (Fig. 4a). The bamboo rings are then bonded with the adhesive to the flax composite skins in a hexagonal packing (Fig. 4b). No adhesive is used between the adjacent bamboo rings. The opposite skin is filled with adhesive and then placed over the bamboo core. Cold bonding is performed by applying a uniform pressure of 3.7 kPa for 24 h at room temperature. The sandwich panels (Fig. 4c) are kept in a plastic bag during the seven days of curing to prevent moisture absorption, and then tested. The dimensions of the sandwiches, obtained according to the ASTM C393 [39], are: 60 mm × 180 mm × 15 mm, for bamboo rings of Ø20 mm and 90 mm × 240 mm × 15 mm, for bamboo rings of Ø30 mm.

2.3. Characterisation

2.3.1. Characterisation of the single material components

The individual material components of the sandwich panels are first characterized in a separate manner. Ten specimens of flax-reinforced composites skins ($0.6 \times 15 \times 250$ mm^3) are tested under tensile loads according to the ASTM D3039 standard [40], at 2 mm/min, by using a 100 kN Instron test machine. Ten single bamboo rings for each diameter (Ø20 and Ø30 mm) are characterised after treatment by compression and density tests (ISO 22157–1 [41] and ISO 22157–2 [42] standards). The compression test is performed at 2 mm/min in a 100 kN Shimadzu AG-X Plus test machine (Fig. 5a), considering bamboo height is twice its outer diameter, i.e., 40 and 60 mm. The strength is determined by the maximum load applied to the cross-sectional area of the hollow tube, i.e., by considering the outer and inner diameter. The density is determined by measuring the dimensions and mass of the bamboos using a calliper and a precision scale. Polymeric adhesives are characterised by ultra-micro dynamic hardness tests (DUH-211S, Shimadzu, Fig. 5b) to evaluate the indentation modulus according to ASTM E2546–15 [43]. Fifteen measurements are performed for each type of adhesive.

2.3.2. Characterisation of the sandwich panels

Sandwich panels are characterised by the three-point bending tests, as shown in Fig. 6. The tests are carried out using a Roell Amsler with

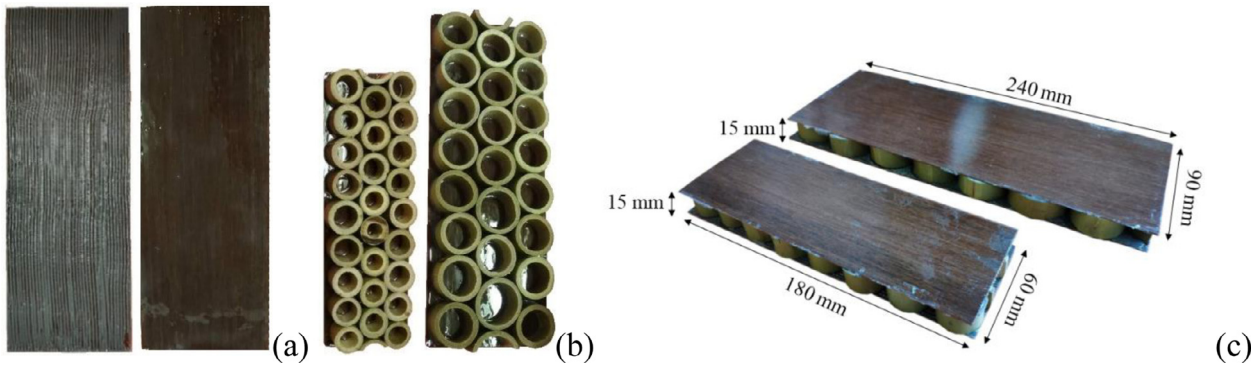

Fig. 4. Sandwich manufacturing process: (a) polymer spread (Left – Huntsman, Right – Sicomin), (b) bonding of bamboo rings (left - Ø20 mm, right - Ø30 mm), (c) sandwich panels.

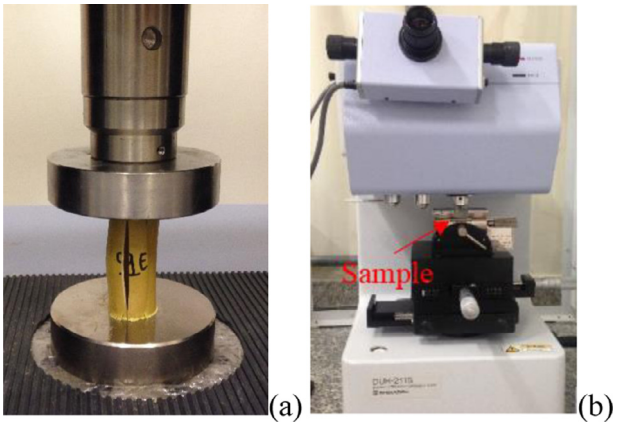

Fig. 5. Characterisation of the single material components: (a) bamboo ring and (b) polymeric adhesives.

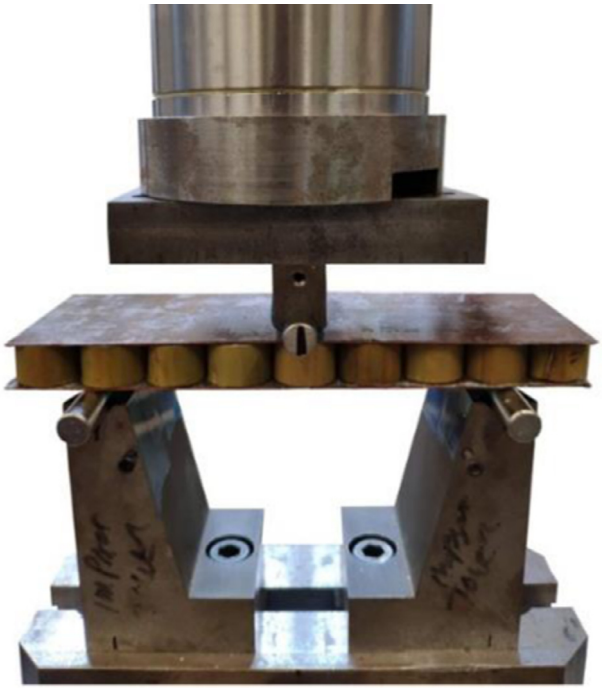

Fig. 6. Characterisation of the sandwich panel via three-point bending test.

a 25 kN load cell at 6 mm/min, with spans of 130 and 190 mm for the sandwich panels made with the Ø20 and Ø30 mm bamboo rings, respectively, according to ASTM C393 [39]. The mechanical responses measured in the test are flexural strength and modulus [44], considering an equivalent homogeneous material; skin stress [39,45]; core shear stress and core shear modulus [7,46]. The equivalent density of the sandwich panels is also assessed by measuring the dimensions and mass of the panels using a calliper and a precision scale.

2.4. Finite element (FE) model

The Finite element (FE) model of sandwich panel under the three-point bending is develop to compare and benchmark against the experimental results. A non-linear FE model is created using the Abaqus™/Standard software version 6.14 in order to obtain the cohesive failure. Fig. 7 shows the 3D representative model of the panel, with the flax skins and bamboo core, which are modelled as orthotropic materials. The engineering constants of the flax reinforced composites are calculated using simplified micromechanics equations reported by Chamis [47] and calibrated based on the elastic modulus (E_T) obtained during the tensile tests. The bamboo engineering constants are obtained based on their microstructural characteristics. Bamboo is known for its sclerenchyma (fibrous phase) and parenchyma constituents [48]. Its cross section shows a fibre bundle gradient that increases the fibre volume fraction from the inner side to outer side. This behaviour changes the mechanical properties along the thickness. The bamboo cross section is therefore divided into three layers (inner, middle and outer) as shown in Fig. 7 (detail A). The inner, middle and outer layers correspond to 60%, 30% and 10% of the total thickness. Different elastic constants calculated according to the fibre volume fraction are assigned to each layer (15 wt% for the inner, 35 wt% for the middle and 50 wt% for the outer layer [49]). The elastics constants of the bamboo layers and flax reinforced composites used in the FE model and their explanation are shown in Table 1. Skins and bamboo are not modelled using failure criteria or degradation law, given that the main failure is debonding between the skins and the bamboo.

A quarter model of the panel is modelled using symmetric boundary conditions to represent the three-point bending. The support and the indenter are modelled as analytical rigid surface (3D rigid surface defined in Abaqus) and fixed to a reference point (RP). Boundary conditions (BCs) are applied to RPs. All displacements and rotations are not allowed in the support RP. All displacements and rotations are also not allowed in the indenter RP except for a maximum imposed displacement of 3 mm along the Y-axys (δ_y). The results of the reaction forces are extracted for the indenter RP and the displacements are monitored in the same point.

Cohesive surfaces are used to model the contact between the skins and the bamboo core. Quadratic traction is used to calculate the failure

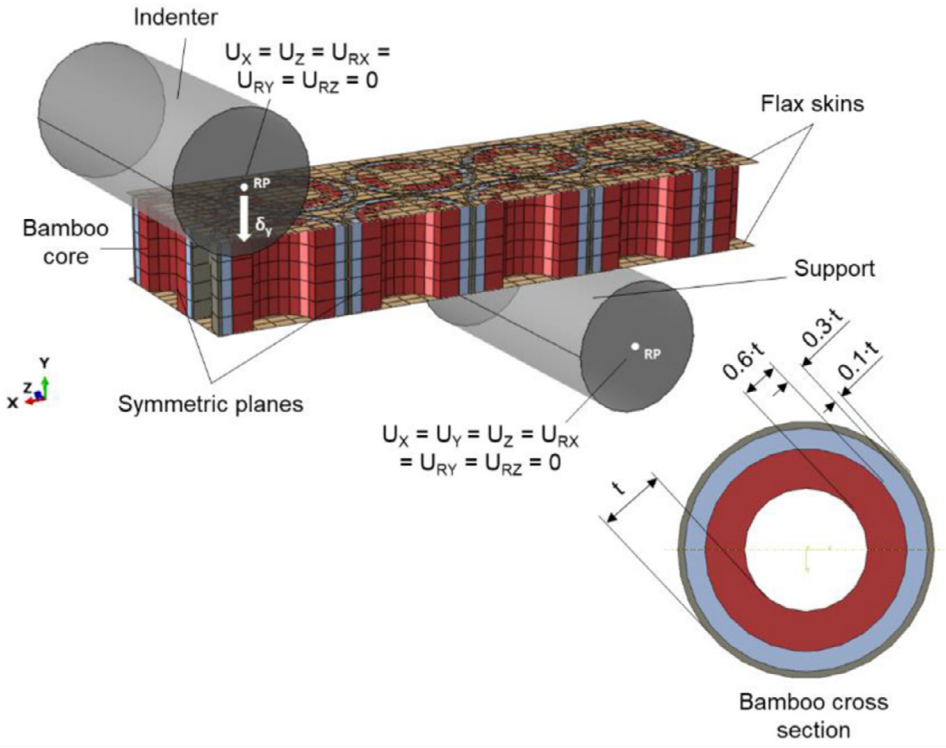

Fig. 7. The 3D FE model used to simulate the three-point bending test: mesh representation, boundary conditions and dimensions.

Table 1
Engineering constants considered in FE model for the phases.

Parameter	Definition	Bamboo			Flax composite
		Inner	Middle	Outer	
E_{11} (GPa)	Longitudinal elastic modulus	6.51	14.98	21.32	34.89
$E_{22} = E_{33}$ (GPa)	Transverse elastic modulus	0.273	0.406	0.560	4.350
$\nu_{12} = \nu_{13} = \nu_{23}$	Poisson's ratio in plane 1–2/1–3/2–3	0.37	0.34	0.31	0.33
$G_{12} = G_{13} = G_{23}$ (GPa)	Shear modulus in plane 1–2/1–3/2–3	0.096	0.141	0.192	4.290

Table 2
Cohesive zone parameters used in the model.

	Direction	Damage initiation stress (N/mm^2)	Fracture energy (N/mm)	Penalty stiffness (N/mm^3)
	Normal	t_{nn}	G_{1c}	K_{nn}
Adhesive	Transverse	$t_{ss} = t_{tt}$	G_{11c}, G_{111c}	K_{ss}, K_{tt}
Huntsman		0.8	0.1	10
Sicomin		1.3	0.1	10

initiation and the degradation of the cohesive surface. Table 2 shows the cohesive zone parameters used in the model. The damage initiation stress parameters are used to establish the initial failure stress along the normal direction (t_{nn}) and the transverse one ($t_{ss} = t_{tt}$). The fracture energy parameters are used to identify the fracture energy along the normal direction (G_{1c}) and the transverse energy (G_{11c}=G_{111c}); penalty stiffness parameters are used to establish the stiffness of the cohesive layer along the normal direction (K_{nn}) and in the transverse one (K_{ss}=K_{tt}). It is well known that these interface properties are totally dependant on the type of adhesive used [50]. Furthermore, it is very difficult to obtain these values in open literature or through mechanical tests for the specific application considered in this work. In view of this, convergence studies are carried out to identify the cohesive zone surfaces from the experiments (Mode I, Mode II and Mixed Mode), based on datasheet of the Huntsman [37] and Sicomin [38] adhesives. The contact between elements of the bamboo core is modelled as normal (frictionless hard and tangential behaviour). In addition, the contacts between the skins and the support and skin/indenter are modelled using normal behaviour, both hard and tangential without friction. Some input parameters, especially cohesive zone are tuned to minimize the gap between experimental and numerical results. The average of the maximum loads obtained during the three-point bending tests are used to calibrate the largest load drop value. Adjustment is performed using two different samples made with the (i) bamboo Ø20 mm/Huntsman adhesive and the (ii) bamboo Ø20 mm/Sicomin adhesive. These two configurations are used to minimize the difference between the experiment and the numerical analysis for the two different types of adhesives used, and then calibrate the overall finite element model.

Flax composite skins are modelled using S4 linear shell elements and three integration points each layer. The bamboo core is meshed using SC8R continuum shell elements. Each layer of bamboo is modelled using one elements through the thickness, resulting in three elements. The mesh convergence study is carried out with three different mesh refinements. The nomenclature used corresponds to the following parameters: l_s/w_s /l_c/d_c, where l_s is the number of elements along the skin length, w_s is the number of the elements along the skin width, l_c is the number of

Table 3
Full Factorial Design (2^2).

Experimental Condition	Bamboo Diameter (mm)	Adhesive Type
1	20	H
2	20	S
3	30	H
4	30	S

elements along the core length and d_c is the number of elements along the core perimeter. The following meshes are used: MESH 1 totalling 1012 elements; MESH 2 with a total of 3000 elements and MESH 3 with 6520 elements. After performing the simulations, the convergence study shows that the results presented using MESH 3 do not differ significantly in relation to the ones from MESH 2. In addition, MESH 3 has a computational time 150% higher when compared to MESH 2. MESH 2 has been, therefore, chosen to perform all analyses.

The main objective of the model is to simulate the bending behaviour (force vs. displacement curve) and to understand the failure mode, and therefore develop a model that can simulate the structural behaviour of this type of sandwich. These results are presented and detailed in Section 3.2.2.

2.5. Statistical experimental design

A full factorial design 2^2 is established to investigate the effect of the bamboo diameter (20 mm / 30 mm) and adhesive type (Huntsman [H] / Sicomin [S]) on the equivalent density, flexural and shear properties of sandwich panels, resulting in four experimental conditions (Table 3). Six specimens (two replicates) are fabricated for each experimental condition, with a total of 24 specimens. The Minitab software v. 18 is used to perform the Design of Experiment (DoE) and Analysis of Variance (ANOVA).

3. Results

3.1. Individual material components of the sandwich panels

Table 4 shows the mechanical and physical properties of the constituents of the sandwich panels. The letters represent the Tukey's comparison test, in which statistically equivalent means (averages) show a similar group of letter. Flax reinforced composites feature a maximum tensile strength and modulus of 313 MPa and 35.8 GPa, respectively. The maximum compressive strength and density are equivalent for the two bamboo diameters (group A). Generally, the mechanical properties vary close to the height of the culm. However, the chosen range (Ø20 – 30 mm) is small to observe major material variations and the results therefore are within the same average, as shown by group A. The compressive modulus is slightly larger for the Ø30 mm bamboo rings. According to open literature [51,52] the fibre volume increases with the culm height, thus, larger diameter bamboo rings (Ø30 mm) have a larger fraction of lignocellusosic matrix and this plays a significant role on matrix-dominated compression properties. The ultra-micro dynamic hardness test shows a superior indentation modulus for the Huntsman (H) adhesive. On the other hand, the density and viscosity of Sycomin (S) adhesive are lower.

3.2. Sandwich panel

Table 5 presents the mean (average) values and standard deviations of the responses related to replicates one and two for the sandwich panels, which are statistically interpreted in Section 3.2.1.

This research involving sustainable sandwich panels made of eco-friendly composite skins and bamboo core is very innovative in the literature. The only similarity found in the literature was reported by Hartoni et al. [35], in which sandwich panels made of plywood skins

Table 4
Mechanical and physical results of the individual material phases of the sandwich panels.

	Tensile		Compressive			Density		Ultra Micro Hardness		Viscosity
	σ_{max} [MPa]	E_T [GPa]	σ_{max} [MPa]		E_C [GPa]	ρ [g/cm^3]		E_{IT} [GPa]		[mPa.s]
Flax reinforced composite	313.01 (±17.88)	35.79 (±2.26)	–		–	–		–		–
Bamboo ring Ø20 mm	–	–	172.11 (±11.12)	A	11.93 (±0.95)	0.904 (±0.029)	B	–		–
Bamboo ring Ø30 mm	–	–	173.95 (±12.03)	A	13.85 (±1.19)	0.925 (±0.048)	A	–		–
Adhesive H	–	–	–		–	1.60*		4.721 (±0.675)	A	90,000* (25 °C)
Adhesive S	–	–	–		–	1.17*		4.213 (±0.393)	B	1620* (20 °C)

* Obtained by the manufacturers [37,38].

Table 5
Mean and standard deviation values for the DoE responses.

	E.C.	Equivalent Density (g/cm^3)	Flexural Strength (MPa)	Flexural Modulus (GPa)	Ultimate skin Stress (MPa)	Ultimate core Shear Stress (MPa)	Core Shear Modulus (MPa)
R1	1	0.491 (±0.019)	6.33 (±0.88)	2.16 (±0.58)	28.28 (±1.73)	0.69 (±0.04)	34.45 (±9.69)
	2	0.470 (±0.008)	8.37 (±0.85)	2.85 (±0.27)	36.98 (±2.19)	0.89 (±0.05)	43.93 (±9.31)
	3	0.404 (±0.004)	9.47 (±0.84)	3.80 (±1.06)	42.40 (±3.24)	0.71 (±0.05)	34.07 (±2.43)
	4	0.390 (±0.009)	11.55 (±1.72)	4.23 (±0.30)	48.95 (±7.96)	0.89 (±0.03)	34.94 (±3.32)
R2	1	0.489 (±0.001)	6.48 (±0.47)	2.16 (±0.64)	26.89 (±4.55)	0.64 (±0.10)	36.48 (±12.24)
	2	0.471 (±0.007)	8.98 (±0.15)	3.07 (±0.72)	35.57 (±3.21)	0.89 (±0.07)	48.13 (±12.29)
	3	0.402 (±0.005)	9.49 (±1.89)	3.43 (±0.21)	39.67 (±7.93)	0.69 (±0.12)	32.73 (±3.25)
	4	0.391 (±0.015)	11.32 (±1.68)	4.24 (±0.41)	47.92 (±7.51)	0.87 (±0.03)	36.60 (±0.62)

Table 6
Characteristics of manufactured sandwich panels.

Type	Bamboo rings per panel	Surface contact area (mm^2)	Non-adhesive area (%)
Sandwich panel Ø20 mm	27	3711.01	65.64
Sandwich panel Ø30 mm	24	5183.63	76.00

Table 7
Analysis of variance (ANOVA).

	Equivalent Density	Flexural Strength	Flexural Modulus	Skin Stress	Core Shear Stress	Core Shear Modulus
Bamboo Diameter (BD)	0.000	**0.000**	**0.000**	**0.000**	0.452	0.005
Adhesive Type (AT)	0.000	**0.000**	**0.003**	**0.001**	**0.000**	0.009
BD x AT	**0.008**	0.393	0.433	0.504	0.199	**0.019**
R^2-adj	99.95%	98.51%	96.62%	97.67%	96.66%	90.26%
Anderson Darling (P-value ≥ 0.05)	0.367	0.819	0.566	0.322	0.989	0.971

and bamboo rings core were tested under three-point bending. The only variable assessed was flexural strength, which ranged from 6 to 10 MPa, being very close to the results obtained in the present study, as shown in Table 5.

Table 6 shows some additional characteristics of the sandwich panels. The percentage of the non-adhesive area is determined by considering the total panel area minus the average surface contact area of the bamboo rings, the whole then divided by the total area of the panel. Twenty-seven (27) bamboo rings of Ø20 mm compose the smaller sandwich panels, resulting in a cross-sectional contact area of 3711 mm^2 and a non-adhesive area of 65.6%. On the other hand, twenty-four (24) bamboo rings of Ø30 mm are used for the larger sandwich panels, resulting in a cross-sectional contact area of 5184 mm^2 and a non-adhesive area of 76%.

3.2.1. Statistical analysis

Table 7 presents the DoE/ANOVA analysis of the responses. Significant effects with P-values less than 0.05, are underlined in Table 7, and those in bold indicate higher-order effects that will be interpreted by the effect plots. The main effect of a factor should only be interpreted individually if there is no other evidence of significant interactions amongst factors. The R^2-adjusted varies from 90.3% to 99.9%, indicating models of high predictability. ANOVA is validated by the Anderson-Darling normality test, where P-values ≥ 0.05 (0.367 – 0.989) imply data of normal distribution.

Equivalent density: The equivalent density of the sandwich panels ranges from 0.390 g/cm^3 (Ø30 mm, adhesive S) to 0.491 g/cm^3 (Ø20 mm, adhesive H). An approximate 4% decrease is observed when the sandwich panel adhesive changes from H to S (Fig. 8); this is attributed to the lower density of the type S adhesive (Table 4). There is also a reduction of 17% when the bamboo diameter changes from Ø20 mm to Ø30 mm. Although the density of the bamboo rings is similar (Table 4, group A), this decrease is due to the smaller number of Ø30 mm bamboo rings per sandwich panel (24) and the greater non-adhesive area (76%) in comparison to the Ø20 mm sandwich panels (Table 6).

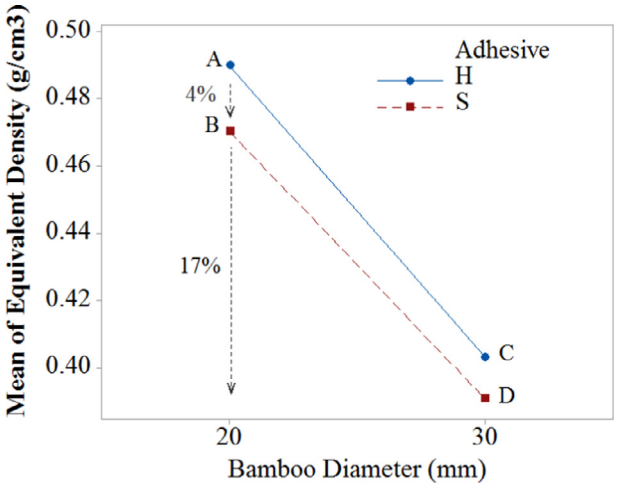

Fig. 8. Second order interaction effect plot for the mean (average) equivalent density.

Bending properties: The flexural strength of the sandwich panels ranges from 6.3 MPa (Ø20 mm, adhesive H) to 11.5 MPa (Ø30 mm, adhesive S). The highest flexural strength is reached for sandwich panels with Ø30 mm bamboo rings and S adhesive, with 39% (Fig. 9a) and 27% (Fig. 9b) increases respectively, when compared to sandwich panels made with the other manufacturing parameters. Although the compressive strength of the two bamboo rings is similar (Table 4, group A), the flexural strength is mainly related to the core-face adhesion. The thickness of the adhesive can affect the quality of the bonding of the panels, which leads to a lower variation when considering a core with fewer bamboo rings (24 rings when designed with Ø30 mm). The adhesive S presents superior results in terms of flexural strength due to its lower viscosity (Table 4); the S adhesive therefore better penetrates in the rough surface of the flax skins and pores of the bamboo rings.

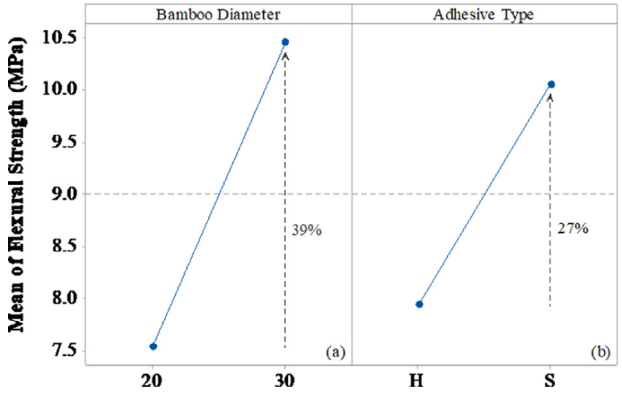

Fig. 9. Main effect plot for the mean (average) flexural strength.

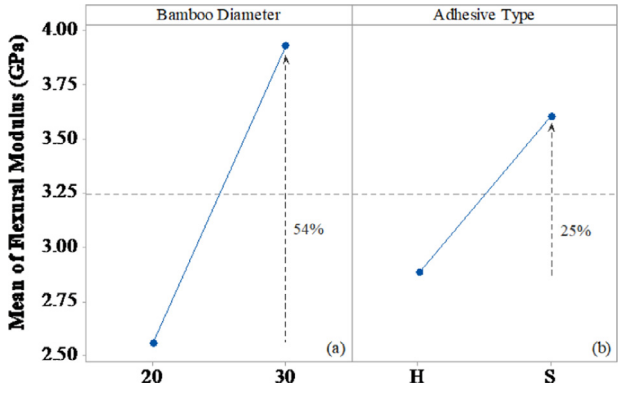

Fig. 10. Main effect plot for the mean (average) flexural modulus.

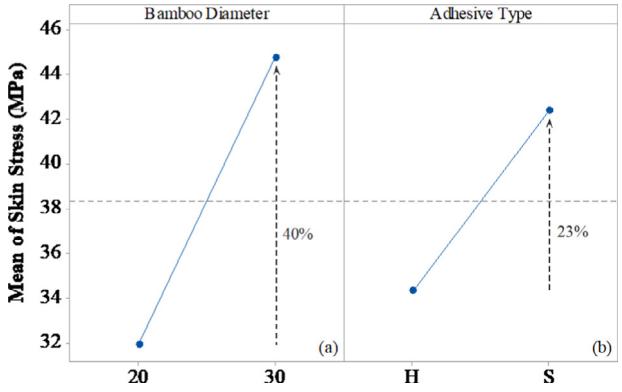

Fig. 11. Main effect plot for the mean (average) skin stress.

The flexural modulus ranges from 2.2 GPa (Ø20 mm, adhesive H) to 4.2 GPa (Ø30 mm, adhesive S). Fig. 10 shows a behaviour similar to the one of the flexural strength, showing increases of 54% and 25% for bamboo rings Ø30 mm and adhesive S, respectively. This increase in modulus for larger bamboo rings is attributed to the higher surface contact area with the polymer (5184 mm^2, Table 5), and this offers higher stiffness and lower deflection during the elastic deformation. Although the H adhesive shows a higher indentation modulus (Table 4), very rigid adhesives can however negatively affect the mechanical performance of the panels, since a brittle adhesive does not follow the deformation of the faces, causing premature cracking and phase debonding.

Skin stress: Skin stress ranges from 26.9 MPa (Ø20 mm, adhesive H) to 48.9 MPa (Ø30 mm, adhesive S). Fig. 11 shows the main effect plots for the average skin stress provided by the bamboo diameters and the type of adhesive used. The graphs show trends similar to the ones related

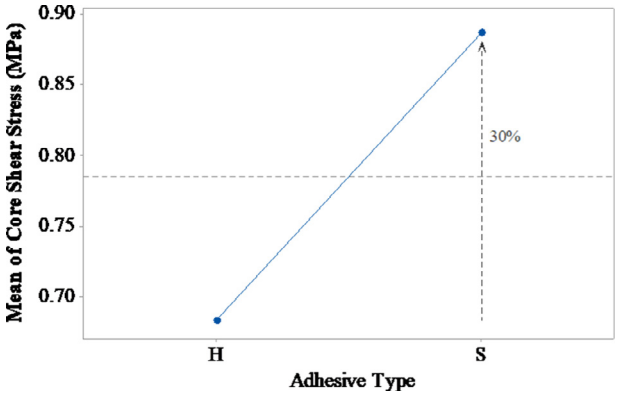

Fig. 12. Main effect plot of adhesive type factor for the mean core shear stress.

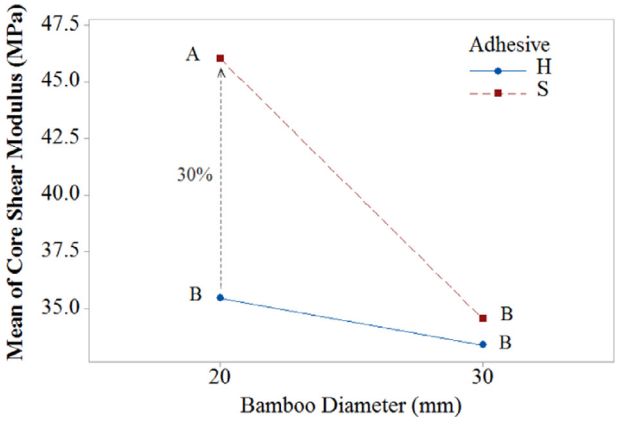

Fig. 13. Second order interaction effect plot for the mean core shear modulus.

to the bending properties, since this response is calculated assuming that the faces take up all the bending load by compressive and tensile forces [45]. Skin stress is directly related to the ability of the skin to withstand the load applied to the panel due to its bonding to the core. A 40% increase of skin stress is observed for Ø30 mm bamboo rings (Fig. 11a) due to the larger surface contact area with the polymer, while an increase of 23% is noted for adhesive S case (Fig. 11b) because of its lower viscosity and higher ductility that improve the bonding of the sandwich panel elements and follows the deformation of the skins.

Shear properties: The core shear stress ranges from 0.64 MPa to 0.89 MPa. Fig. 12 shows the main effect plot of the adhesive type factor for the mean core shear stress. The core shear stress is closely related to the mechanical properties of the core constituents and their bonding to the faces. Since the two bamboo rings present similar compressive stress and modulus, only the specific type of adhesive used significantly affects this response, with a 30% increase when adhesive S is considered. This fact can be attributed to the lower viscosity and rigidity of this type of adhesive (see Table 4), which improves the core-face adhesion and longer creep-like deformations; the elements therefore tend to bond for longer and avoid the onset of premature cracks in the sandwich beam.

The core shear modulus ranges from 32.7 MPa (Ø30 mm, adhesive H) to 48.1 MPa (Ø20 mm, adhesive S). An opposite behaviour to bending is observed for this response in terms of the diameter effect (Fig. 13). Smaller bamboo diameters offer higher shear rigidity due to the larger number of bamboo rings per area and higher adhesive area, which increases the shear constraints, especially when the S adhesive is used. This result also implies that the higher ductility of the S-adhesive and the larger number of Ø20 mm bamboo rings lead to a positive interaction effect that increases the core shear modulus of the panels. Panels made with H-adhesive or Ø30 mm rings with S-adhesive reach equivalent means evidenced by group B (Tukey test).

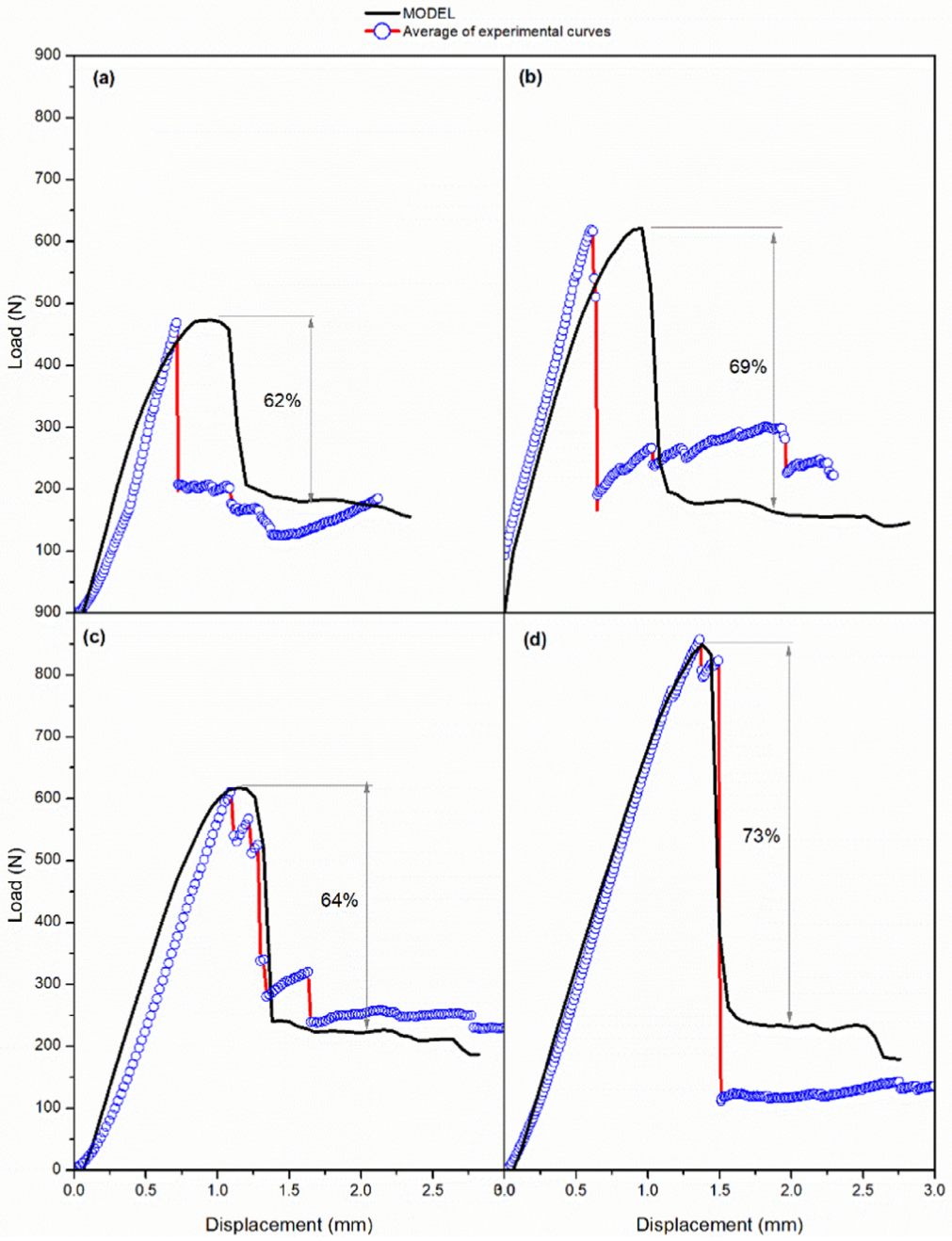

Fig. 14. Load versus displacement curves in three point bending test for experimental conditions: (a) H – 20 mm, (b) S – 20 mm, (c) H – 30 mm and (d) S – 30 mm.

3.2.2. Experimental and numerical comparisons

Fig. 14 shows the load versus displacement curves obtained by the three-point bending tests (average of experimental curves) and the finite element model for all experimental conditions. A similar trend is noted, which is described by a long elastic deformation with adhesive crack initiation, followed by a sudden drop. The highest flexural strength occurs in the S - 30 mm sample (Condition 4), followed by the S - 20 mm (Condition 2), H - 30 mm (Condition 3) and H - 20 mm (Condition 1) samples. A good match between the numerical and experimental model is evident in the initial and linear part of the curves. The results also show a good level of adjustment of the mechanical properties and constituents imparted on the model, mainly in relation to the division of the bamboo cross section into three layers. The model also predicts the drop load of the curves after the maximum load, with the presence of a subsequent residual strength in the numerical and experimental results. The damage is quantified in terms of maximum load, dividing the average residual load by the maximum one. As expected, the structure damage increases when the maximum load increases. In addition, although the model considers a local condition, due to the method used in the implementation, such as symmetry conditions and simplified mesh elements, it uses a full-scale model for sandwich applications in structural conditions.

Fig. 15a shows the state of the samples after failure in the experimental tests and Fig. 15b shows the shape deformation in the numerical model. Mirroring is applied to the model symmetry planes for an improved visualization. Similar failure in all conditions are found, where the sudden drop in the force-displacement curves is caused by debonding between the face and the adhesive. This behaviour shows that the failure criteria and the degradation law in the cohesive elements are activated. In general, the onset of debonding mainly occurs on the bot-

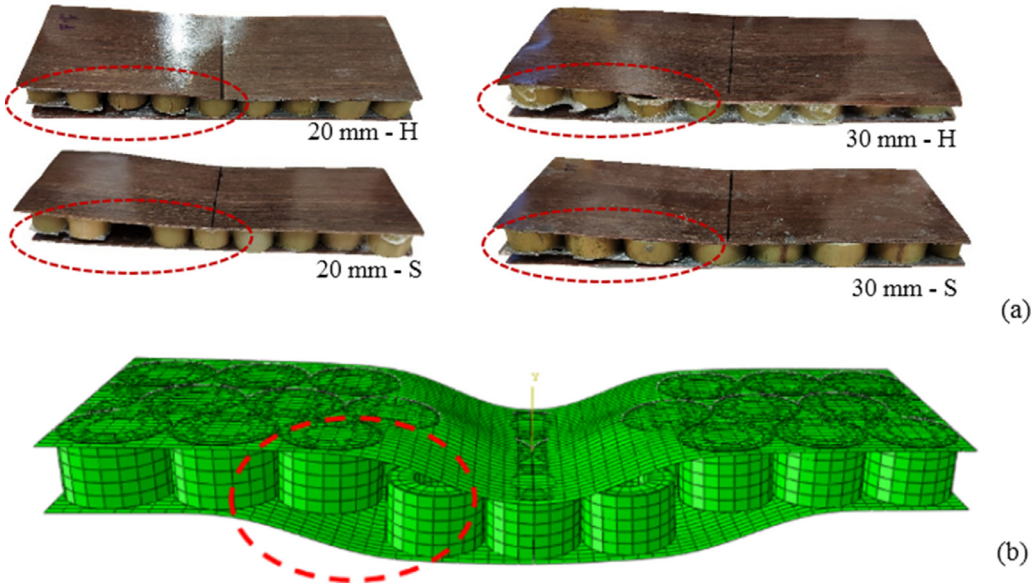

Fig. 15. The failure mode of the sandwich panels: (a) experimental and (b) shape deformation in the numerical model.

tom skin, but in some cases it also occurs on the top surfaces due to the buckling effect of the skins, leading to interfacial pull-out stresses. Some panels also reveal a loss of the bamboo ring, as shown in Fig. 15a for the Ø20 mm – S panels. This failure mode also shows a better bamboo-polymer bonding rather than skin-polymer one, which is explained by the presence of porosity in the bamboo cross section that favours an improved interlocking effect. The numerical results also show a similar failure behaviour when compared to the experimental ones. Debonding is mostly found between the bottom skin and the bamboo.

4. Conclusions

Sustainable sandwich panels made of unidirectional prepreg flax skins and bamboo rings as circular core material are here developed, characterised and investigated through a statistical experimental design and a finite element model. The effects of adhesive type and bamboo diameter on the equivalent density, flexural and shear properties of the panels are identified. The main conclusions of this work are the following: i. The equivalent density of the sandwich panels is affected not only by the density of the adhesive, but mainly by the percentage of non-adhesive area in the core, resulting in a decrease when larger bamboo rings (Ø30 mm) are used; ii. The sandwich panels with Ø30 mm bamboo rings have a higher superficial contact area with the adhesive, resulting in better core-face bonding with higher flexural properties and skin stress. In contrast, the sandwich panels made with the Ø20 mm bamboo rings reveal an increase in the core shear modulus due to the larger number of bamboo rings per area and higher adhesive area, increasing shear constraints; iii. The type S adhesive has a lower viscosity and indentation modulus, which positively affects all responses, increasing skin stress, bending and shear properties; iv. All experimental conditions exhibit debonding between the bottom skin and the adhesive, indicating that the polymeric adhesive plays an important role in the mechanical performance of the sandwich panels. v. The finite element model predicts a good match in terms of load versus displacement curves. The modelling using three-layer bamboo cross sections (inner, middle and outer) and the use of ortotropic properties provides a good agreement with the stiffness of the structure. In addition, the cohesive surface elements provide a substantially correct prediction of the failure and type of damages. The model corroborates the experimental data, which show that the main failure mode of the panels is the debonding between the skin and the bamboo rings.

Finally, the sandwich panels reveal a promising application for secondary structural components, where low cost, moderate stresses and biodegradable characteristics are required, expanding the horizons of the future of sustainable engineering structures.

Declaration of Competing Interest

The authors declare that there is no conflict of interest.

Acknowledgements

LAdO and THP are grateful to the Bristol Composites Institute (ACCIS) and the University of Bristol for the logistic support provided during the manufacturing and testing of the panels. The authors would like to thank SSUCHY for the flaxtape supply, the Brazilian Research Agencies, CAPES (PhD scholarship) and CNPq (PQ 309885/2019-1), for the financial support provided.

References

[1] N.O. Cabrera, B. Alcock, T. Peijs, Design and manufacture of all-PP sandwich panels based on co-extruded polypropylene tapes, Compos. Part. B-Eng 39 (2008) 1183–1195, doi:10.1016/j.compositesb.2008.03.010.
[2] L.L. Hu, X.L. He, G.P. Wu, T.X. Yu, Dynamic crushing of the circular-celled honeycombs under out-of-plane impact, Inter. J. Impact Eng 75 (2015) 150–161, doi:10.1016/j.ijimpeng.2014.08.008.
[3] M. Gholami, R.A. Alashti, A. Fathi, Optimal design of a honeycomb core composite sandwich panel using evolutionary optimization algorithms, Compos. Struct. 139 (2016) 254–262, doi:10.1016/j.compstruct.2015.12.019.
[4] Z. Wang, J. Liu, D. Hui, Mechanical behaviors of inclined cell honeycomb structure subjected to compression, Compos. Part B-Eng. 110 (2017) 307–314, doi:10.1016/j.compositesb.2016.10.062.
[5] Z. Wang, Z. Li, W. Zhou, D. Hui, On the influence of structural defects for honeycomb structure, Compos. Part B-Eng. 142 (2018) 183–192, doi:10.1016/j.compositesb.2018.01.015.
[6] Z. Wang, Z. Li, W. Xiong, Experimental investigation on bending behavior of honeycomb sandwich panel with ceramic tile face-sheet, Compos. Part B-Eng. 164 (2019) 280–286, doi:10.1016/j.compositesb.2018.10.077.
[7] H.G. Allen, Analysis and Design of Structural Sandwich Panels, Pergamon Press, 1969.
[8] R.J. D'Mello, A.M. Waas, Synergistic energy absorption in the axial crush response of filled circular cell honeycombs, Compos. Struct. 94 (2012) 1669–1676.
[9] P.R. Oliveira, A.M.S. Bonaccorsi, T.H. Panzera, A.L. Christoforo A.L, F. Scarpa, Sustainable sandwich composite structures made from aluminium sheets and disposed bottle caps, Thin Wall. Struct. 120 (2017) 38–45, doi:10.1016/j.tws.2017.08.013.
[10] J.R. Dutra, S.L.M.R Filho, A.L. Christoforo, T.H. Panzera, F. Scarpa, Investigations on sustainable honeycomb sandwich panels containing eucalyptus sawdust. Piassava and cement particles, Thin Wall. Struct (2019) 143, doi:10.1016/j.tws.2019.106191.

[11] J. Smardzewski, Wooden sandwich panels with prismatic core – Energy absorbing capabilities, Compos. Struct. (2019) 230, doi:10.1016/j..compstruct.2019.111535.
[12] M. Ramesh, K. Palanikumar, K.H. Reddy, Plant fibre based bio-composites: sustainable and renewable green materials, Renew. Sust. Energ. Rev 79 (2017) 558–584, doi:10.1016/j.rser.2017.05.094.
[13] H. Ku, H. Wang, N. Pattarachaiyakoop, M. Trada, A review on the tensile properties of natural fiber reinforced polymer composites, Compos. Part B-Eng. 42 (2011) 856–873, doi:10.1016/j.compositesb.2011.01.010.
[14] K.L. Pickering, M.G.A. Efendy, T.M. Le, A review of recent developments in natural fibre composites and their mechanical performance, Compos. Part A. 83 (2016) 98–112, doi:10.1016/j.compositesa.2015.08.038.
[15] A. Regazzi, S. Corn, P. Ienny, A. Bergeret, Coupled hydro-mechanical aging of short flax fiber reinforced composites, Polym. Degrad. Stabil. 130 (2016) 300–306, doi:10.1016/j.polymdegradstab.2016.06.016.
[16] V. Fiore, T. Scalici, D. Badagliacco, D. Enea, G. Alaimo, A. Valenza, Aging resistance of bio-epoxy jute-basalt hybrid composites as novel multilayer structures for cladding, Compos. Struct. 160 (2017) 1319–1328, doi:10.1016/j.compstruct.2016.11.025.
[17] V. Fiore, L. Calabrese, G. Di Bella, T. Scalici, G. Galtieri, A. Valenza, Proverbio E, Effects of aging in salt spray conditions on flax and flax/basalt reinforced composites: wettability and dynamic mechanical properties, Compos. Part B-Eng. 93 (2016) 35–42, doi:10.1016/j.compositesb.2016.02.057.
[18] M. Ramesh, Flax (Linum usitatissimum L.) fire reinforced polymer composite materials: a review on preparation, properties and prospects, Prog. Mater. Sci. 102 (2019) 109–166, doi:10.1016/j.pmatsci.2018.12.004.
[19] I. Zivkovic, C. Fragassa, A. Pavlovic, T. Brugo, Influence of moisture absorption on the impact properties of flax, basalt and hybrid flax/basalt fiber reinforced green composites, Compos. Part B-Eng. 111 (2017) 148–164, doi:10.1016/j.compositesb.2016.12.018.
[20] L. Yan, N. Chouw, K. Jayaraman, Flax fibre and its composites – a review, Compos Part B-Eng 56 (2014) 296–317, doi:10.1016/j.compositesb.2013.08.014.
[21] Available in: https://eco-technilin.com/en/ (2019).
[22] W.-t. Li, Y.-l. Long, J. Huang, Y. Lin, Axial load behavior of structural bamboo filled with concrete and cement mortar, Constr. Build. Mater. 148 (2017) 273–287, doi:10.1016/j.conbuildmat.2017.05.061.
[23] P.-h. Lee, M. Odlin, H. Yin, Development of a hollow cylinder test for the elastic modulus distribution and the ultimate strength of bamboo, Constr. Build. Mater. 51 (2014) 235–243, doi:10.1016/j.conbuildmat.2013.10.051.
[24] H.-t. Li, J.-w. Su, Q.-s. Zhang, A.J. Deeks, D. Hui, Mechanical performance of laminated bamboo column under axial compression, Compos. Part B-Eng 79 (2015) 374–382, doi:10.1016/j.compositesb.2015.04.027.
[25] J.Q. Krause, F.A. Silva, K. Ghavami, O.F.M. Gomes, R.D.T. Filho, On the influence of *Dendrocalamus giganteus* bamboo microstructure on its mechanical behavior, Constr. Build. Mater. 127 (2016) 199–209, doi:10.1016/j.conbuildmat.2016.09.104.
[26] S. Jakovljevic, D. Lisjak, Z. Alar, F. Penava, The influence of humidity on mechanical properties of bamboo for bicycles, Constr. Build. Mater. 150 (2017) 35–48, doi:10.1016/j.conbuildmat.2017.05.189.
[27] B. Cen, Y. Liu, Z. Zeng, J. Wang, X. Lu, X. Zhu, Mechanical behavior of novel GFRP foam sandwich adhesive joints, Compos. Part B-Eng. 130 (2017) 1–10, doi:10.1016/j.compositesb.2017.07.034.
[28] A. Calik, Effect of adherend shape on stress concentration reduction of adhesively bonded single lap joint, Eng. Rev. 36 (2016) 29–34.
[29] N.R.E. Domingues, R.D.S.G. Campilho, R.J.C. Carbas, L.F.M. da Silva, Experimental and numerical failure analysis of aluminium/composite single-L joints, Int. J. Adhes. Adhes. 64 (2016) 86–96, doi:10.1016/j.ijadhadh.2015.10.011.
[30] A.J. Kinloch, J.H. Lee, A.C. Taylor, S. Sprenger, C. Eger, D. Egan, Toughening structural adhesives via nano and micro-phase inclusions, J. Adhes. 79 (2003) 867–873, doi:10.1080/00218460309551.
[31] J.J. Garcia, R. Christian, G. Khosrow, Experiments with rings to determine the anisotropic elastic constants of bamboo, Constr. Build. Mater. 31 (2012) 52–57, doi:10.1016/j.conbuildmat.2011.12.089.
[32] M.D.E. Candelaria, J.Y. Hernandez Jr, Determination of the properties of bambusa blumeana using full-culm compression tests and layered tensile tests for finite element model simulation using orthotropic material modeling, ASEAN Eng. J. 9 (2019) 54–71.
[33] E.C.N. Silva, M.C. Walters, G.H. Paulino, Modeling bamboo as a functionally graded material: lessons for the analysis of affordable materials, J. Mater. Sci. 41 (2006) 6991–7004, doi:10.1007/s10853-006-0232-3.
[34] S. Darzi, H. Karampour, B.P. Gilbert, H. Bailleres, Numerical study on the flexural capacity of ultra-light composite timber sandwich panels, Compos. Part B-Eng. 155 (2018) 212–224, doi:10.1016/j.compositesb.2018.08.022.
[35] J.Fajrin Hartoni, B. Anshari, Effect of core and skin thicknesses of bamboo sandwich composite on bending strength, Int. J. Mech. Eng. Tech. 8 (2017) 551–560.
[36] A. Loth, R. Föster, Comboo - a novel core material for composite sandwich structures from renewable sources, in: Proceedings of the 18th European Conference on Composite Materials - ECCM18, 2018.
[37] Available in: http://dms.etra.fi:9000/19572646/fi/master?1466175672000 (2004).
[38] Available in: http://www.sicomin.com/datasheets/product-pdf1154.pdf (2018).
[39] ASTM C393/C393M – 16, Standard test method for core shear properties of sandwich constructions by beam flexure (2016).
[40] ASTM D3039/3039M – 17, Standard test method for tensile properties of polymer matrix composite materials (2017).
[41] ISO 22157 – 1, Bamboo – Determination of physical and mechanical properties – Part 1: requirements (2004).
[42] ISO 22157 – 2, Bamboo – Determination of physical and mechanical properties – Part 2: laboratory manual (2004).
[43] ASTM E2546 – 15, Standard test method for tensile properties of polymer matrix composite materials (2015).
[44] ASTM D790 – 15, Standard test methods for flexural properties of unreinforced and reinforced plastics and electrical insulating materials (2015).
[45] T. Bitzer, Honeycomb Technology: Materials, Design, Manufacturing, Applications and Testing, Springer, 1997.
[46] ASTM D7250/D7250M – 16, Standard test method for determining sandwich beam flexural and shear stiffness (2016).
[47] C.C. Chamis, Simplified composite micromechanics for predicting microstresses, J. Reinf. Plast. Comp. 6 (1987) 268–289, doi:10.1177/073168448700600305.
[48] F.L. Palombini, W. Kindlein Jr., B.F. Oliveira, J.E.A. Mariath, Bionics and design: 3D microstructural characterization and numerical analysis of bamboo based on X-ray microtomography, Mater. Charact. 120 (2016) 357–368, doi:10.1016/j.matchar.2016.09.022.
[49] P.G. Dixon, L.T. Gibson, The structure and mechanics of Moso bamboo material, J. R. Soc. Interface. 11 (2014) 1–12, doi:10.1098/rsif.2014.0321.
[50] I. Katsivalis, O.T. Thomsen, S. Feih, M. Achintha, Development of cohesive zone models for the prediction of damage and failure of glass/steel adhesive joints, Int. J. Adhes. Adhes. 97 (2020) 1–10, doi:10.1016/j.ijadhadh.2019.102479.
[51] J. Gottron, K.A. Harries, Q. Xu, Creep behaviour of bamboo, Constr. Build. Mater. 66 (2014) 79–88, doi:10.1016/j.conbuildmat.2014.05.024.
[52] Q. Xu, K. Harries, X. Li, Q. Liu, J. Gottron, Mechanical properties of structural bamboo following immersion in water, Eng. Struct. 81 (2014) 230–239, doi:10.1016/j.engstruct.2014.09.044.